DOI 10.24425/aee.2023.145422

A new method for estimating fault location in radial medium voltage distribution network only using measurements at feeder beginning

TRUONG NGOC-HUNG

Department of I.T., FPT University – Quy Nhon A.I Campus
Dong Da ward, Quy Nhon city, Viet Nam
e-mail: hungtn19@fe.edu.vn

(Received: 25.12.2022, revised: 13.02.2023)

Abstract: This paper proposes a new fault location method in radial medium voltage distribution networks. The proposed method only uses the measurement data at the feeder beginning to approximate the characteristic equation showing the dependence between the positive-sequence voltage and phase angle at the monitoring point with the distance to the fault location for each fault type on each line segment. To determine these characteristic equation coefficients, the entire distribution network will be modeled and simulated by four types of faults at different locations along the lines to build the initial database. Based on this database, the mathematical functions in MATLAB software are applied to approximate these coefficients corresponding to each type of fault for each line segment in the network. Then, from the current and voltage measurement data at the feeder beginning, the algorithms of global search, comparison, and fault ranking are used to find out where the fault occurs on the distribution network. Two types of distribution network with and without branches are studied and simulated in this paper to verify and evaluate the effectiveness of the proposed method.

Key words: characteristic equation, distribution network, fault location, fault ranking index, global search

1. Introduction

The distribution network has the main task of supplying power to the loads for ensuring power quality and reliability [1]. A medium voltage distribution network usually has voltage levels of 6, 10, 15, 22, and 35 kV to supply power to medium/low voltage distribution substations

and medium voltage loads. A distribution network typically has a radial or ring connection configuration in the same source substation or multiple source substations together [2]. Although there is a ring connection, most of medium voltage distribution networks operate at an open-loop status. As a result, the open-loop operation leads to power loss and voltage quality poorer than the closed-loop operation, it has many advantages such as: cheap grid investment, simple switchgear, and relay protection requirements, etc. A distribution network has a ring connection with many different power substations with the help of electronic computers and remote-control systems that allow us to operate the network economically in the normal state and flexibly in the situation of failure, contributing to ensuring high reliability level. The cut-off point for the open-loop operation is changed frequently during operation when the load graph changes, the optimal operation diagram is calculated from the telemetry data located at the locations on the grid. When a fault occurs on the network, the control center will also determine the best alternative operation plan. The operator implements optimal diagrams with remote control devices [3].

For a distribution network, the main components for calculating and applying the fault location method are operating parameters of the network, techniques to determine the fault location that needs many measurement points on the network. When smart grid technology and distributed generations are involved in the current network operation, it is very important to detect and locate fault accurately [4]. The lack of direct measurement points on the distribution network becomes a major challenge for fault analysis. However, the smart grid technology is evolving with the use of modern equipment such as the advanced metering infrastructure (AMI), smart electronic device (IED) and other devices that provide measurement data for more efficient fault analysis. Modern recloser controllers perform the communications for remote control and fault and power quality analysis. These devices store data in a sequence of remotely accessed faults.

Many techniques are used to locate fault on the distribution networks [5, 6] as well as the transmission networks [7–9]. Those techniques are classified into two basic categories: the signal processing techniques [10–12] and knowledge base-based techniques [13, 14] as shown in Fig. 1.

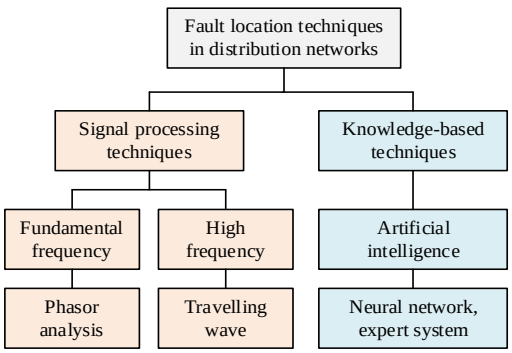

Fig. 1. Fault location overview

The knowledge-based techniques need a large database to train the network [15]. In the work [16], the general classification of fault location techniques for the distribution networks is

presented. In the work [17], the impedance method was used to locate the fault in the distribution networks. In the work [18], the data is collected from the fault index along the network when the fault is predetermined.

The authors in [19] proposed a new method for fault location based on system analysis at non-fundamental frequencies. Solving optimization problem using genetic algorithm based on calculating voltage changes was proposed for fault location in distribution network by the work [20]. The new method based on an ensemble learning was proposed in the work [21] for fault location in a smart distribution network. The work [22] proposed an improved algorithm for fault location in radial distribution system using discrete and continuous wavelet analysis. Furthermore, the fault location problem in distribution networks with distributed generations was solved by a new method based on the impedance matrix [23], the information about the fault provided by directional fault passage indicators and intelligent electronic devices [24], and the high frequency impedance [25]. The measurements provided by the smart meters are used in a state estimation method for fault location in distribution networks [26]. The synchronized/non-synchronized measurements were used for locating faults in smart distribution networks [27] as well as in transmission lines with a static var compensator [28]. In addition, the new methods based on the zero-sequence component characteristic [29] and based on the modal analysis [30] were proposed for fault location in distribution networks. The authors in [31] applied an impedance-based method to design and implement a real-time fault location experimental system for teaching and training universities in which voltage and current measurements at the monitoring point are recorded to determine the distance to the fault. The approach based on the phasor measurement of a real digital fault recorder was proposed in [32]. This method was developed for transmission lines, and it has the advantage of providing a reliable search field which can be utilized to optimize line inspection procedures.

This paper proposes a new fault location method on radial medium voltage distribution networks based on the voltage magnitude and phase angle measurements at the monitoring point when a fault occurs on the network. The characteristic equations showing the relationship between the positive sequence voltage magnitude and phase angle at the monitoring point are established from the fault simulation database set on the distribution network by the MATLAB/Simulink software. These characteristic equations are established for each fault type for all segments on the network. They are the basis to determine the fault location on the network. Two network types with and without sub-feeders were modeled and simulated to build an initial database to establish the characteristic equation between the positive sequence voltage magnitude and phase angle with the distance to fault. The new contributions of this paper are shown in the following key points:

(i) Establish the characteristic equations showing the dependence of the positive sequence voltage magnitude and phase angle at the monitoring point according to the distance to fault. This is done based on building a database of the distribution network on MATLAB/Simulink software and simulating faults alone the feeders in the network.

(ii) Rank the faulty segments by the global search algorithm to determine the exact fault location on the faulty one of the distribution networks with sub-feeders. This fault ranking index is determined based on the difference between the positive sequence voltage magnitude distance and the positive sequence phase angle distance.

2. Fault location methods for distribution networks

2.1. Fault analysis background

To locate fault in radial distribution networks, we need to analyze the different fault types. The fault analysis of a three-phase distribution network is performed by the symmetrical component method [3] and modeled by a reduced electric circuit as shown in Fig. 2, where the fault can occur at one of the five locations denoted by the black dots.

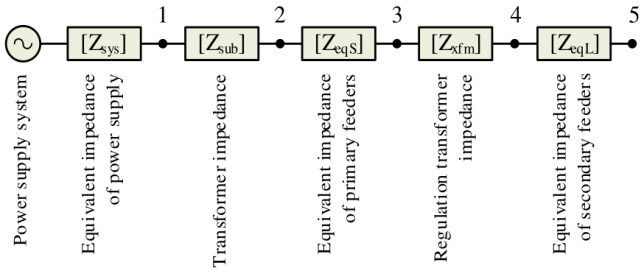

Fig. 2. Fault analysis model of distribution network

The three-phase and one-phase short-circuit power values at the point 1 are considered as the specifications for modeling the power system at the transmission grid level. The positive sequence equivalent impedance Z_+ of the power system is determined according to the three-phase short-circuit power as follows [3]:

$$Z_+ = \frac{U^2}{S^*_{3\phi}}, \tag{1}$$

where: U is the line voltage, $S_{3\phi}$ is the three-phase short-circuit power of the system and the symbol * is the complex number.

Similarly, the zero-sequence equivalent impedance Z_0 of the system is determined according to the single-phase short-circuit power as follows [3]:

$$Z_0 = \frac{3U^2}{S^*_{1\phi}} - 2Z_+, \tag{2}$$

where $S_{1\phi}$ is the single-phase short-circuit power of the system.

Using the predetermined positive- and zero-sequence impedances, the component impedance matrix is defined by the following equation [3]:

$$Z_{\text{seq}} = \begin{bmatrix} Z_0 & 0 & 0 \\ 0 & Z_+ & 0 \\ 0 & 0 & Z_+ \end{bmatrix}. \tag{3}$$

The equivalent impedance matrix is determined as follows [3]:

$$Z_{\text{eq}} = \frac{1}{3}\begin{bmatrix} 2Z_+ + Z_0 & Z_0 - Z_+ & Z_0 - Z_+ \\ Z_0 - Z_+ & 2Z_+ + Z_0 & Z_0 - Z_+ \\ Z_0 - Z_+ & Z_0 - Z_+ & 2Z_+ + Z_0 \end{bmatrix}. \tag{4}$$

The fault location at the points 2, 3, 4, and 5 are calculated based on the three-phase to ground fault and the Thevenin's law at the fault location. Figure 3 shows the equivalent electric circuit according to the Thevenin's law viewed from the fault location of the network, where U_a, U_b, and U_c are the phase voltages at the monitoring point and they are determined according to Eq. (5). According to the Thevenin's law, the total phase impedance matrix at the fault location is determined by the total impedance Z_{total}, the variable Z_f being the fault impedance.

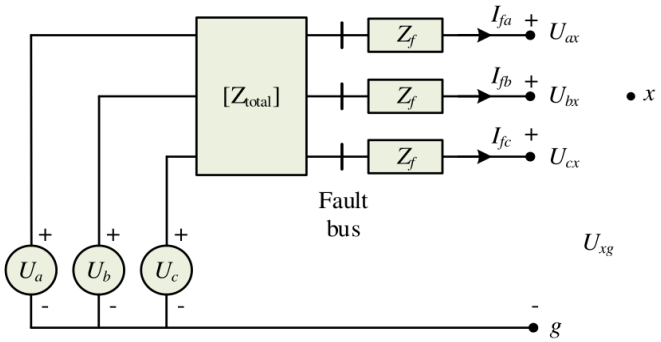

Fig. 3. Equivalent model for fault analysis

$$\begin{bmatrix} U_a \\ U_b \\ U_c \end{bmatrix} = \begin{bmatrix} Z_{aa} & Z_{ab} & Z_{ac} \\ Z_{ba} & Z_{bb} & Z_{bc} \\ Z_{ca} & Z_{cb} & Z_{cc} \end{bmatrix} \begin{bmatrix} I_{fa} \\ I_{fb} \\ I_{fc} \end{bmatrix} + \begin{bmatrix} Z_f & 0 & 0 \\ 0 & Z_f & 0 \\ 0 & 0 & Z_f \end{bmatrix} \begin{bmatrix} I_{fa} \\ I_{fb} \\ I_{fc} \end{bmatrix} + \begin{bmatrix} U_{ax} \\ U_{bx} \\ U_{cx} \end{bmatrix} + \begin{bmatrix} U_{xg} \\ U_{xg} \\ U_{xg} \end{bmatrix}. \tag{5}$$

In Eq. (5) there are seven unknown variables to be calculated which are: I_{fa}, I_{fb}, I_{fc}, U_{ax}, U_{bx}, U_{cx}, and U_{xg}. Equation (5) shows three equations containing the relationship between those variables. To find the above seven variables, it is necessary to add the remaining equations that they are determined based on the characteristic of each fault type including: three-phase to ground (LLLG) fault, line-to-line (LL) fault, line-to-line to ground (LLG) fault and single-phase to ground (LG) fault [7]. The fault impedance Z_f in (5) represents the fault impedance path between phase or ground faults [33] and it is not considered an unknown variable in (5). However, the fault impedance is an undefined input parameter depending on the arc resistance of the fault. In this work, the fault impedance is assumed by 0 Ω for four fault types to establish the database and the build the characteristic of each fault type. Besides, the fault impedance is selected by 0, 5, 10, and 15 Ω in the second case study to verify the proposed method.

2.2. The proposed fault location method

This paper uses a radial medium voltage distribution network as shown in Fig. 4 to propose the new fault location method. On this network, the voltage and current measurement devices are installed at the monitoring point (bus 2) – the source busbar. If a fault occurs at any segment of the network, the changes of voltage and current are measured and stored at the monitoring point [34]. These changes are to reduce the voltage magnitude and to vary the voltage phase angle. Furthermore, these changes have different characteristic, and they are stored by the intelligent

electronic devices (IEDs) at the monitoring point. Based on the characteristic equations, the fault location is estimated by analyzing and comparing between the voltage measurements at the source busbar and the database. The database can be built up from the practical data or from the simulation data of the distribution network. Due to the complexity and difficulty of building up the database from the practical data, this paper studies to build up the database from the simulation data via the MATLAB/Simulink environment. The simulation data is then used to determine the characteristic equation coefficients as well as to calculate the distance to fault on the network for each location fault.

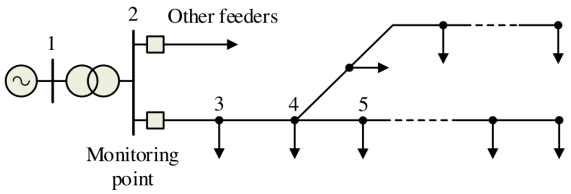

Fig. 4. Studied distribution network configuration

Two types of typical database are used for the proposed method. *The first* one is the voltage magnitude and phase angle measured during a fault at all buses. The stored voltage magnitude is the lowest value among the three phase voltage magnitudes. *The second* one is a characteristic equation of the positive sequence voltage magnitude and phase angle as a function of the distance to fault, these equations are considered as the positive sequence voltage magnitude and phase angle measured at the source substation busbar. Different fault types will have different databases. These databases are represented as Table 1: the first column is the fault location on the network, the second one is the fault type, the third one is the phase-A voltage magnitude, the fourth one is the phase-A phase angle, the fifth one is the phase-B voltage magnitude, the sixth one is the phase-B phase angle, the seventh one is the phase-C voltage magnitude, the eighth one is the phase-C phase angle, the ninth one is the positive sequence voltage magnitude, the tenth one is the positive sequence phase angle.

The above analysis shows that there are three forms showing the relationship between the positive sequence voltage magnitude and phase angle with the distance to fault: *linear form, nonlinear form, and constant form*. Each form has its own equation depending on the grid impedance [1]. For the large impedance will change more non-linearly, in other words the small impedance will make the characteristic linear and all constant. In this paper, the characteristic equation used is the form of the fifth-order equation in the general form [32, 34]:

$$U_+ = a_5 d^5 + a_4 d^4 + a_3 d^3 + a_2 d^2 + a_1 d + a_0, \tag{6}$$

$$\theta_+ = b_5 d^5 + b_4 d^4 + b_3 d^3 + b_2 d^2 + b_1 d + b_0, \tag{7}$$

where: U_+ is the positive sequence voltage magnitude at the source busbar location, θ_+ is the positive sequence phase angle at the source busbar location, d is the distance from the source busbar to the fault location, a_n $(n = 0, 1, 2, 3, 4, 5)$ is the coefficient of the positive sequence voltage magnitude equation, b_n $(n = 0, 1, 2, 3, 4, 5)$ is the coefficient of the positive sequence phase angle equation, respectively.

Table 1. Typical record data of faulty feeder

Fault location (km)	**Fault type**	U_a	θ_a	U_b	θ_b	U_c	θ_c	U_+	θ_+
1	LG	$U_a^{(1)}$	$\theta_a^{(1)}$	$U_b^{(1)}$	$\theta_b^{(1)}$	$U_c^{(1)}$	$\theta_c^{(1)}$	$U_+^{(1)}$	$\theta_+^{(1)}$
	LL	$U_a^{(2)}$	$\theta_a^{(2)}$	$U_b^{(2)}$	$\theta_b^{(2)}$	$U_c^{(2)}$	$\theta_c^{(2)}$	$U_+^{(2)}$	$\theta_+^{(2)}$
	LLG	$U_a^{(1,1)}$	$\theta_a^{(1,1)}$	$U_b^{(1,1)}$	$\theta_b^{(1,1)}$	$U_c^{(1,1)}$	$\theta_c^{(1,1)}$	$U_+^{(1,1)}$	$\theta_+^{(1,1)}$
	LLLG	$U_a^{(2)}$	$\theta_a^{(2)}$	$U_b^{(2)}$	$\theta_b^{(2)}$	$U_c^{(2)}$	$\theta_c^{(2)}$	$U_+^{(2)}$	$\theta_+^{(2)}$
2	LG	$U_a^{(1)}$	$\theta_a^{(1)}$	$U_b^{(1)}$	$\theta_b^{(1)}$	$U_c^{(1)}$	$\theta_c^{(1)}$	$U_+^{(1)}$	$\theta_+^{(1)}$
	LL	$U_a^{(2)}$	$\theta_a^{(2)}$	$U_b^{(2)}$	$\theta_b^{(2)}$	$U_c^{(2)}$	$\theta_c^{(2)}$	$U_+^{(2)}$	$\theta_+^{(2)}$
	LLG	$U_a^{(1,1)}$	$\theta_a^{(1,1)}$	$U_b^{(1,1)}$	$\theta_b^{(1,1)}$	$U_c^{(1,1)}$	$\theta_c^{(1,1)}$	$U_+^{(1,1)}$	$\theta_+^{(1,1)}$
	LLLG	$U_a^{(2)}$	$\theta_a^{(2)}$	$U_b^{(2)}$	$\theta_b^{(2)}$	$U_c^{(2)}$	$\theta_c^{(2)}$	$U_+^{(2)}$	$\theta_+^{(2)}$
⋮	⋮	⋮	⋮	⋮	⋮	⋮	⋮	⋮	⋮
x	LG	$U_{a,x}^{(1)}$	$\theta_{a,x}^{(1)}$	$U_{b,x}^{(1)}$	$\theta_{b,x}^{(1)}$	$U_{c,x}^{(1)}$	$\theta_{c,x}^{(1)}$	$U_{+,x}^{(1)}$	$\theta_{+,x}^{(1)}$
	LL	$U_{a,x}^{(2)}$	$\theta_{a,x}^{(2)}$	$U_{b,x}^{(2)}$	$\theta_{b,x}^{(2)}$	$U_{c,x}^{(2)}$	$\theta_{c,x}^{(2)}$	$U_{+,x}^{(2)}$	$\theta_{+,x}^{(2)}$
	LLG	$U_{a,x}^{(1,1)}$	$\theta_{a,x}^{(1,1)}$	$U_{b,x}^{(1,1)}$	$\theta_{b,x}^{(1,1)}$	$U_{c,x}^{(1,1)}$	$\theta_{c,x}^{(1,1)}$	$U_{+,x}^{(1,1)}$	$\theta_{+,x}^{(1,1)}$
	LLLG	$U_{a,x}^{(2)}$	$\theta_{a,x}^{(2)}$	$U_{b,x}^{(2)}$	$\theta_{b,x}^{(2)}$	$U_{c,x}^{(2)}$	$\theta_{c,x}^{(2)}$	$U_{+,x}^{(2)}$	$\theta_{+,x}^{(2)}$

The constant values a_n and b_n depend on the form of the characteristic equation as follows:

(i) Nonlinear form – all the coefficients in Eqs. (6) and (7) are non-zero.

(ii) Linear form – the coefficients b_5 is none-zero and the remaining coefficients equal zero.

(iii) Constant form – only the coefficients a_0 and b_0 are non-zero and the remaining coefficients equal 0.

The arrangement of the data in two forms of the database such as Tables 2 and 3. In these two data tables, the first column is the segment from the bus i to the bus j, the second, third, fourth, fifth, sixth, and seventh columns are the characteristic equation coefficients (6) and (7).

Table 2. Characteristic equation coefficients of positive sequence voltage by distance

Segment	a_5	a_4	a_3	a_2	a_1	a_0
2–3	a_5^{2-3}	a_4^{2-3}	a_3^{2-3}	a_2^{2-3}	a_1^{2-3}	a_0^{2-3}
3–4	a_5^{3-4}	a_4^{3-4}	a_3^{3-4}	a_2^{3-4}	a_1^{3-4}	a_0^{3-4}
4–5	a_5^{4-5}	a_4^{4-5}	a_3^{4-5}	a_2^{4-5}	a_1^{4-5}	a_0^{4-5}
⋮	⋮	⋮	⋮	⋮	⋮	⋮
i–j	a_5^{i-j}	a_4^{i-j}	a_3^{i-j}	a_2^{i-j}	a_1^{i-j}	a_0^{i-j}

The data search used to construct the proposed algorithm is performed as Fig. 5. The positive sequence voltage magnitude and phase angle measurements at the monitoring point are used

Table 3. Characteristic equation coefficients of positive sequence phase angle by distance

Segment	b_5	b_4	b_3	b_2	b_1	b_0
2–3	b_5^{2-3}	b_4^{2-3}	b_3^{2-3}	b_2^{2-3}	b_1^{2-3}	b_0^{2-3}
3–4	b_5^{3-4}	b_4^{3-4}	b_3^{3-4}	b_2^{3-4}	b_1^{3-4}	b_0^{3-4}
4–5	b_5^{4-5}	b_4^{4-5}	b_3^{4-5}	b_2^{4-5}	b_1^{4-5}	b_0^{4-5}
⋮	⋮	⋮	⋮	⋮	⋮	⋮
i–*j*	b_5^{i-j}	b_4^{i-j}	b_3^{i-j}	b_2^{i-j}	b_1^{i-j}	b_0^{i-j}

as the input data to carry out the next steps. In Fig. 5, the purpose of the global search is to identify all segments that are likely to occur fault with the results of the positive sequence voltage magnitude and phase angle at the monitoring point (U_+, θ_+). After running the global search, the measurement values are compared with the positive sequence voltage magnitude and phase angle results from the characteristic Eqs. (6) and (7) to determine the distances d_u and d_θ. Then the proposed method determines the difference value between d_u and d_θ to conduct the fault ranking of the segments that are likely to occur fault. Finally, based on this fault ranking index to locate fault in the distribution network.

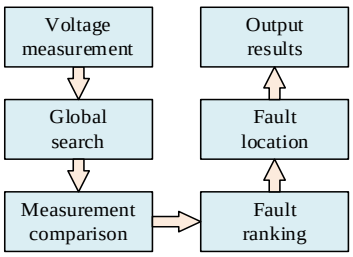

Fig. 5. Proposed method flowchart

It is assumed that a fault occurs on the segment from the bus i to the bus j of the radial distribution network, the fault range is shown by the yellow area on Fig. 6. This range represents

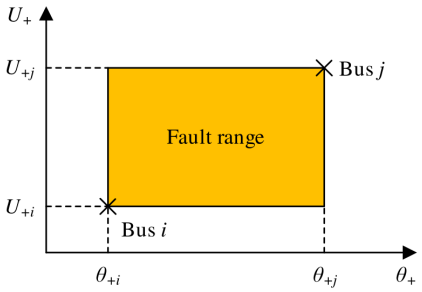

Fig. 6. Fault range from bus i to bus j

the boundary of the positive sequence voltage magnitude and phase angle at the monitoring point corresponding to the fault occurrence at any location on the segment ij and is determined according to characteristic Eqs. (8), (9), and (10). The positive sequence voltage magnitude and phase angle of that range shall be considered as the faulty segment. Each segment in the network has its own range but they are also likely to overlap, that overlap makes appearing many faulty segments. As a result, the global search algorithm is applied to find out the faulty segment correctly.

$$\text{If } U_{+i} < U_+ < U_{+j} \quad \text{and } \theta_{+i} < \theta_+ < \theta_{+j} \quad \text{then fault locaion is between bus } i \text{ and } j, \tag{8}$$

$$\text{If } |U_+ - U_{+i}| < \alpha \quad \text{and } |\theta_+ - \theta_{+i}| < \alpha \quad \text{then fault location is bus } i, \tag{9}$$

$$\text{If } \left|U_+ - U_{+j}\right| < \alpha \quad \text{and } \left|\theta_+ - \theta_{+j}\right| < \alpha \quad \text{then fault location is bus } j, \tag{10}$$

where α is the predetermined threshold for comparing the actual value and the simulation result – the threshold required because the absolute accuracy cannot be achieved. Based on the value recorded at the monitoring point and based on the characteristic equation of the positive sequence voltage magnitude and phase angle by distance (6) and (7) to determine the fault location. Figure 7 shows the distance to fault based on the characteristic equation to find out the fault location on the segment. In addition, Fig. 7 also shows the relation between the characteristic equation of the positive sequence voltage magnitude by distance shown as $U_+ = f_u(d, \text{type})$ and the positive sequence phase angle by distance shown as $\theta_+ = f_\theta(d, \text{type})$.

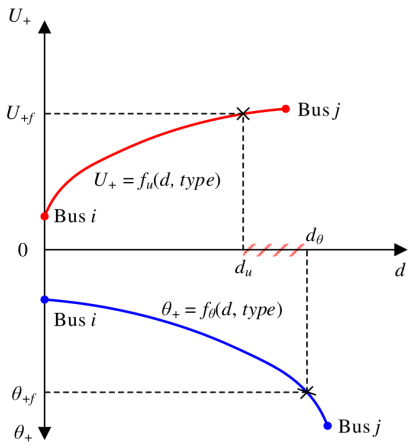

Fig. 7. The curves showing the positive sequence voltage and phase angle characteristic equations

Observed in Fig. 7, although the fault occurs at a location on the segment from the bus i to the bus j, the distance to fault is determined by the positive sequence voltage magnitude (d_u) and by the positive sequence phase angle (d_θ) may be different. That difference value is determined according to Eq. (11), and it is also a value for ranking the faulty segments in this proposed method.

$$\sigma = |d_u - d_\theta|, \tag{11}$$

where σ is the difference between the voltage distance d_u and the phase angle distance d_θ. If many segments can appear fault from the global search algorithm, the difference σ is used to find out the fault ranking index for each segment by Eq. (12). As a result, the segment which is ranked by the value of 1 is the segment occurs fault on it.

$$\sigma_{\min} = \min\{\sigma_1, \sigma_2, \cdots, \sigma_k\} \quad (1 < k < n), \tag{12}$$

where: n is the number of segments which are selected from the global search data, k is the k-the segment in the set of global search data.

3. Simulation results and discussion

For modeling and simulating the case studies in this paper, MATLAB/Simulink is applied to carry out the simulation results. MATLAB/Simulink is a graphical programming environment for modeling, simulating, and analyzing multi-domain dynamical systems. It is widely used in automatic control and digital signal processing for multi-domain simulation and model-based design [35]. The microprocessor used to install MATLAB/Simulink in this work has the specifications of Intel(R) Core (TM) i5 CPU M520 @ 2.40 GHz. The radial medium voltage distribution feeders are modeled and simulated in MATLAB/Simulink by using the solver type of fixed-step discrete solver with the sampling time of 10^{-5} s. The two following cases are studied to verify the effectiveness of the proposed method of this work.

3.1. Case 1

For case 1, this paper applies the proposed fault location method to the simple medium voltage feeder as shown in Fig. 8. The 22 kV feeder from the bus 2 to the bus 3 is received electric at the bus 1 via the transformer substation 110/22 kV to supply power for the load at the end of the feeder. The feeder parameters include: the length $L = 20$ km, the positive sequence impedance $\Omega Z_+ = 0.2459 + j0.3449$ km, the zero-sequence impedance $Z_0 = 0.3939 + j1.6012$ Ω/km. The 110 kV power supply source inner impedance is $Z_S = 0.1694 + j0.484$ Ω/km. The transformer ratings are 25 MVA and 110/22 kV. The load at the bus 3 is $S_{\text{load}} = 300 + j150$ kVA. This distribution network is modeled and simulated in the MATLAB/Simulink environment. Four fault types: three-phase to ground (LLLG) fault, line-to-line (LL) fault, line-to-line to ground (LLG) fault, and single-phase to ground (LG) fault are established at locations alone the feeder. For this 20 km feeder, the fault locations with a fault resistance of 0 Ω are assumed at every two kilometers on the feeder; therefore, 10 locations are simulated with four fault types to record the

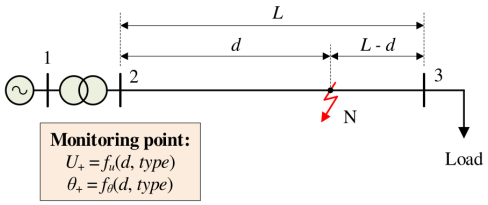

Fig. 8. The feeder of case 1

measurement data at the feeder beginning. As a result, the voltage magnitude and phase angle at the bus 2 of each fault type are stored as in Table 1. This paper uses then the positive sequence voltage and phase angle in Table 1 to determine the coefficients a_n in (6) and b_n in (7) for each fault type. These coefficients a_n and b_n in this case are calculated and given in Table 4 (for the voltage characteristic equation coefficients) and Table 5 (for the phase angle characteristic equation coefficients).

Table 4. Characteristic equation coefficients of positive sequence voltage in case 1

Faulty segment	Fault type	a_5	a_4	a_3	a_2	a_1	a_0
2–3(Z_f = 0 Ω))	LG	0	0	0.0007	–0.0093	0.0671	0.748
	LL	0	0	0.0003	–0.0057	0.0674	0.553
	LLG	0	0	0.0008	–0.0125	0.1142	0.396
	LLLG	0	0	0.0011	–0.0179	0.1698	0.024

Table 5. Characteristic equation coefficients of positive sequence phase angle in case 1

Faulty segment	Fault type	b_5	b_4	b_3	b_2	b_1	b_0
2–3(Z_f = 0 Ω)	LG	0	0.0002	–0.0048	0.0463	–0.0701	–2.1620
	LL	0	0.0013	–0.0322	0.3688	–1.7057	–3.4553
	LLG	0	0.0011	–0.0262	0.2820	–1.0036	–6.4867
	LLLG	0	–0.0012	0.0356	–0.5531	5.2255	–33.6193

The relation between the positive sequence voltage and phase angle by the distance to fault is shown in Fig. 9(a) (for the voltage) and Fig. 9(b) (for the phase angle). Each fault type is represented by a characteristic curve and shown clearly in these two figures. The points marked

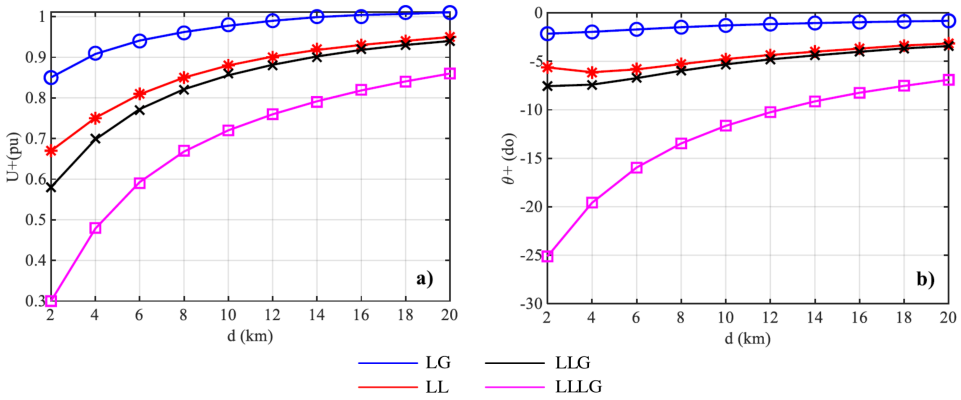

Fig. 9. Simulation results of case 1: (a) characteristic curve of positive sequence voltage by distance; (b) characteristic curve of positive sequence phase angle by distance

by the symbols: "o", "*", "x", and "□" are determined by the values of (U_+, d) and (θ_+, d) at the asummed fault locations alone the feeder length. It is clearly that the points "o", "*", "x", and "□" of each fault type track on its characteristic curve. As a result, if a fault occurs at a location on the feeder, the values of the positive sequence voltage and phase angle at the monitoring point are used as well as the characteristic Eqs. (6) and (7) to estimate the distance to fault. The distance to fault is determined by the voltage characteristic equation d_u and by the phase angle characteristic equation d_θ. The two values d_u and d_θ are used to estimate the distance to fault on the feeder.

3.2. Case 2

To evaluate the effectiviness of the proposed method for real radial medium voltage distribution networks, this case uses a network configuration as shown in Fig. 10 to model and simulate in the Matlab/Simulink environment. The detailed element parameters of this network are presented in Table 6. All feeders of this network are supplied power by a transformer substation 110/22 kV and the source busbar at the bus 2 is considered as the monitoring point; therefore, the voltage and current measurement data at the bus 2 are recorded and stored when a fault occurs on the network. On the other hand, two sub-feeders originated from the bus 4 consist of the segments 4–5 and 4–6. The voltage and phase angle measurement data at the bus 2 for four fault types (LLLG, LL, LLG, and LG) on the segments: 2–3, 3–4, 4–5, and 4–6 are simulated to initialize the database of the whole network. Furthermore, the database is also stored by a specific structure as in Tables 2 and 3. The proposed method uses the data column of the positive sequence magnitude and phase angle in these tables to determine the characteristics equation coefficients a_n and b_n for the main feeder and sub-feeders of the network.

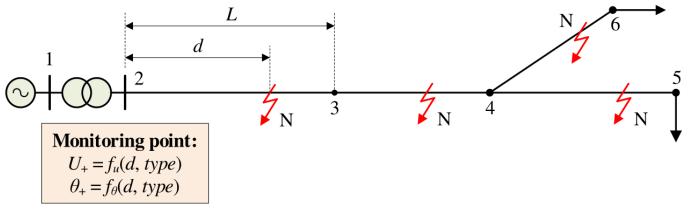

Fig. 10. The feeder of case 2

The characteristics equations showing the relation between the positive sequence voltage magnitude and phase angle by the distance to fault for the main feeder 2–3–4 in this case are given by the curves as shown in Fig. 11(a) (for the positive sequence voltage magnitude) and Fig. 11(b) (for the positive sequence phase angle). These results show that if the fault location is far from the source busbar, the voltage magnitude and phase angle are high because of the dependance on the impedance from the source busbar to the fault location. From the characteristics curves of positive sequence voltage magnitude and phase angle, the distance to fault can be estimated correctly and quickly for each fault type on any segment of the network. This advantage is confirmed by the simulation results for fault locations on the segments 2–3 and 3–4 which are presented at the end of this subsection.

From the simulation database of the network in case 2, the characteristics equations showing the relation between the positive sequence voltage magnitude and phase angle by the distance

Table 6. The detailed element parameters of the feeder of case 2

No.	Element	Parameter
1	Source	The nominal phase-to-phase voltage U_n = 110 kV The nominal frequency f_n = 50 Hz The inner impedance $Z_s = 0.0847 + j0.2420\ \Omega$
2	Power transformer	The nominal power S_n = 25 MVA; The nominal phase-to-phase voltages U_{n1}/U_{n2} = 110/22 kV Winding impedance $Z = 0.00151 + j0.11234$ pu Magnetization impedance $Z_m = 500 + j500\ pu$
3	Segment 2–3	Length L = 10 km Positive sequence impedance $\Omega Z_+ = 0.2459 + j0.3449\,/\text{km}$ Zero sequence impedance $\Omega Z_0 = 0.3939 + j1.6012\,/\text{km}$
4	Segment 3–4	Length L = 10 km Positive sequence impedance $\Omega Z_+ = 0.2459 + j0.3449\,/\text{km}$ Zero sequence impedance $\Omega Z_0 = 0.3939 + j1.6012\,/\text{km}$
5	Segment 4–5	Length L = 10 km Positive sequence impedance $\Omega Z_+ = 0.2459 + j0.3449\,/\text{km}$ Zero sequence impedance $\Omega Z_0 = 0.3939 + j1.6012\,/\text{km}$
6	Load 5	Nominal phase-to-phase voltage U_n = 22 kV Nominal frequency f_n = 50 Hz Active power P = 300 kW Inductive reactive power Q_L = 150 kvar
7	Load 6	Nominal phase-to-phase voltage U_n = 22 kV Nominal frequency f_n = 50 Hz Active power P = 300 kW Inductive reactive power Q_L = 150 kvar

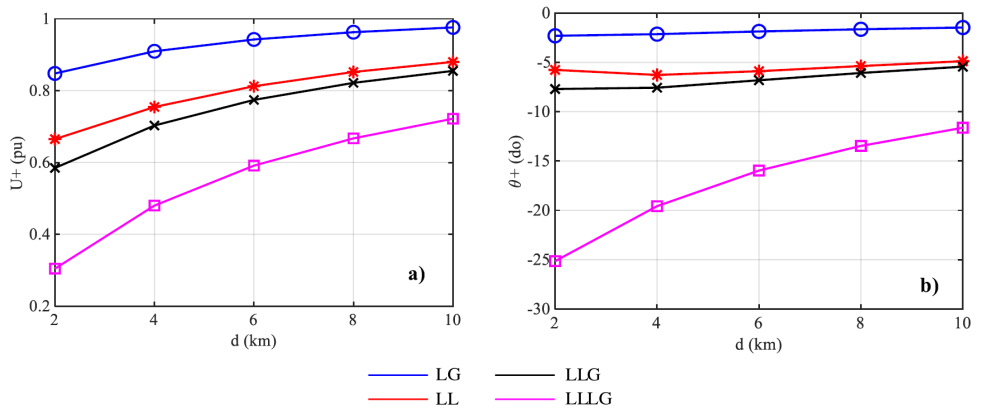

Fig. 11. Simulation results for main feeder of case 2: (a) characteristic curve of positive sequence voltage by distance; (b) characteristic curve of positive sequence phase angle by distance

to fault on the sub-feeders 4–5 and 4–6 are established. These equations are also considered as an useful tool to estimate the fault location on the sub-feeders. Figure 12(a) shows the positive sequence voltage magnitude characteristics curve and Fig. 12(b) shows the positive sequence phase angle characteristics curve. However, these curves are stored in the Matlab environment by the coeficients a_n and b_n to estimate easily the values of distance to fault: d_u and d_θ when the voltage measurements at the source busbar is recorded and stored as the input data of the proposed method.

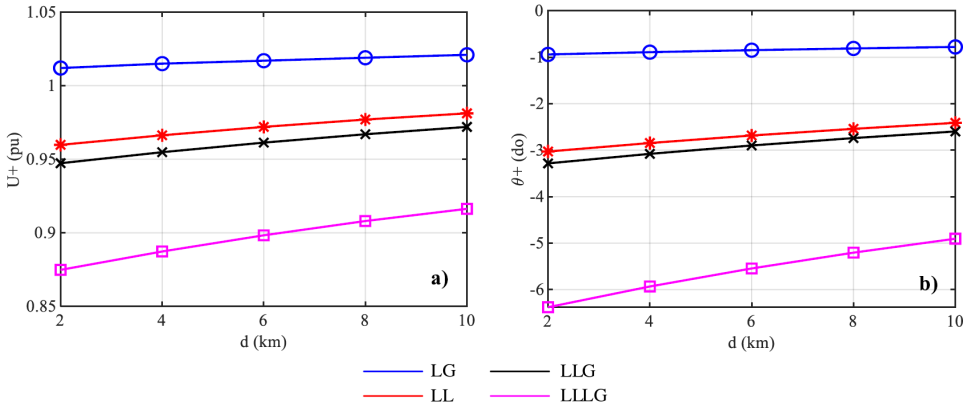

Fig. 12. Simulation results for other feeder of case 2: (a) characteristic curve of positive sequence voltage by distance; (b) characteristic curve of positive sequence phase angle by distance

After determining all the characteristics equation coeficients for the positive sequence voltage magnitude and phase angle of all segments in the network, the paper assumed four fault locations which occur on the segments: 2–3, 3–4, 4–5, and 4–6 as shown in Table 7 to evaluate the effectiveness of the proposed method as presented in Section 2. In these four fault locations, the first two locations are on the main feeder of the network: segment 2–3 with a fault resistance of 0 Ω and segment 3–4 with a fault resistance of 5 Ω, but the last two locations are on the sub-feeders of the network: segment 4–5 with a fault resistance of 10 Ω and segment 4–6 with a fault resistance of 15 Ω. For each fault location as in Table 7, the voltage magnitude and phase angle measurements at the bus 2 are recorded and stored, the characteristics equations established from the simulation results of the whole network are then used to estimate the distance to fault.

Table 7. The scenarios for evaluating the proposed fault location method

No.	Fault segment	Fault location on the feeder	Fault impedance
1	2–3	0.50 pu (distance from bus 2)	Z_f = 0 Ω
2	3–4	0.75 pu (distance from bus 3)	Z_f = 5 Ω
3	4–5	0.65 pu (distance from bus 4)	Z_f = 10 Ω
4	4–6	0.25 pu (distance from bus 4)	Z_f = 15 Ω

The simulation results for evaluating the proposed method of the network in case 2 are given in Table 8. In Table 8, the first column is the numerical order, the second one shows the faulty segments, the third and fourth ones present the distance estimations from the voltage magnitude characteristics equation (d_u) and the phase angle characteristics equation (d_θ), respectively, the fifth column is the distance difference (σ) between the values d_u and d_θ, the last column is the fault ranking index of the faulty segment. The results in Table 8 helps to estimate correctly the fault location on the radial medium voltage distribution network. Moreover, the fault ranking for the main feeder is high accuracy, for example: for the segment 2–3, the fault location is determined at 0.5 pu distance from the bus 2 (d_u = 0.49634 pu and d_θ = 0.49644) pu; similarly, for the segment 3–4, the fault location is also determined correctly at 0.75 pu distance from the bus 3 (d_u = 0.75203 pu and d_θ = 0.75184 pu). On the other hand, for the fault location on the segment 4–5 at 0.65 pu distance from the bus 4, the proposed method gives two faulty segments including 4–5 and 4–6; therefore, the global search algorithm is applied to rank the faulty segment by calculating the fault ranking index (σ). Observing Table 8, the fault ranking index of the faulty segment 4–5 (σ = 0.00085) pu is lower than the index of the faulty segment 4–6 (σ = 0.00143) pu. As a result, the faulty segment 4–5 is ranked by the index of 1 and the faulty segment 4–6 is ranked by the index of 2. This confirms that the fault location is on the segment 4–5 at 0.65 pu distance from bus 4. Similarly, for the fault location on the segment 4–6 at 0.25 pu distance from the bus 4, the proposed method finds out two faulty segments: 4–5 and 4–6. However, the fault ranking index of the faulty segment 4–6 σ = 0.00006 pu is lower than the index of the faulty segment 4–5 (σ = 0.00151 pu), the faulty segment 4–6 is ranked by the index of 1 and the faulty segment 4–5 is ranked by the index of 2. This confirms that the fault location is on the segment 4–6 at 0.25 pu distance from the bus 4.

Table 8. Fault ranking indexes of case 2

No.	Fault segment	d_u (pu)	d_θ (pu)	σ (pu)	Ranking index
1	2–3	0.49634	0.49644	0.00010	**1**
2	3–4	0.75203	0.75184	0.00019	**1**
3	4–5	0.65015	0.65100	0.00085	**1**
	4–6	0.64980	0.65123	0.00143	2
4	4–6	0.25314	0.25308	0.00006	**1**
	4–5	0.25169	0.25323	0.00151	2

The simulation results of case 2 show that the proposed method has accurately located the fault location on the radial medium-voltage distribution network. The method is based in the model of the entire grid on MATLAB/Simulink software and simulation database in four fault types with a fault impedance of 0 Ω to establish the characteristic equations of positive sequence voltage magnitude and phase angle. Then, several fault locations with nonzero fault impedance values are simulated to evaluate the effectiveness of the proposed method. The research results are clearly shown in Table 8. However, one disadvantage of the proposed method is that it is still limited if the fault impedance is large, and the fault location is far from the power source point

because the capacitive component of the line will affect the positive sequence voltage magnitude and phase angle. As a result, the errors d_u and d_θ in Fig. 7 will be large making the fault location no longer accurate. Therefore, future research work will combine the advantages of the proposed method with the support of the SCADA system to overcome this disadvantage.

4. Conclusions

Ensuring power quality and reliability is one of the most important tasks for operating distribution networks; therefore, studying fault location in distribution networks is very essential to reduce long power interruption duration for electric customers. This paper proposed the fault location method based on the measurement data at the monitoring point. This method uses the fault simulation data of the network to approximate the characteristic equations showing the dependance of positive sequence magnitude and phase angle by the distance to fault for each fault type. The real measurement data at the monitoring point will be recorded by the intelligent digital equipment as well as will be used to estimate the distance to fault.

For the case of having many faulty segments, to correctly determine the segment which appears the fault, the global search calculates the fault ranking indexes of each segment. As a result, the segment with the fault ranking index of 1 is the fault one. Furthermore, the fault location on the faulty segment is also estimated from the distance errors d_u and d_θ. The proposed method will be developed in the future to exploit the advantages of the supervisory control and data acquisition (SCADA) system at the control center to correctly find fault areas and improve the network's operating performance. In addition, all the status variables of the devices on the distribution network are used to support restoring the network after occurring the fault.

Acknowledgements

This work is (partly) supported by the research project No. DHFPT/2022/18 granted by FPT University.

References

[1] Mokryani G., *Future Distribution Networks: Planning, Operation, and Control*, AIP Publishing (2022), DOI: 10.1063/9780735422339.

[2] Kezunovic M., *Smart Fault Location for Smart Grids*, IEEE Transactions on Smart Grid, vol. 2, no. 1, pp. 11–22 (2011), DOI: 10.1109/TSG.2011.2118774.

[3] Lampley G.C., *Fault analysis on electrical distribution system*, in IEEE Rural Electric Power Conference, Charleston, SC, USA (2008), DOI: 10.1109/REPCON.2008.4520142.

[4] Liang J., Jing T., Niu H., Wang J., *Two-Terminal Fault Location Method of Distribution Network Based on Adaptive Convolution Neural Network*, IEEE Access, vol. 8, pp. 54035–54043 (2020), DOI: 10.1109/ACCESS.2020.2980573.

[5] Liu L., *Faulted feeder identification and location for a single line-to-ground fault in ungrounded distribution system based on principal frequency component*, Archives of Electrical Engineering, vol. 69, no. 3, pp. 695–704 (2020), DOI: 10.24425/aee.2020.133926.

[6] Menchafou Y., Zahri M., Habibi M., Markhi H.E., *Optimal load distribution estimation for fault location in electric power distribution systems*, Archives of Electrical Engineering, vol. 66, no. 1, pp. 77–87 (2017), DOI: 10.1515/aee-2017-0006.

[7] Saha M.M., Izykowski J.J., Rosolowski E., *Fault Location on Power Networks*, Springer Science and Business Media (2009), DOI: 10.1007/978-1-84882-886-5.

[8] Salim R.H., Resener M., Filomena A.D., Oliveira K.R.C., Bretas A.S., *Extended Fault-Location Formulation for Power Distribution Systems*, IEEE Transactions on Power Delivery, vol. 24, no. 2, pp. 508–516 (2009), DOI: 10.1109/TPWRD.2008.2002977.

[9] Zhang Y., Bi A., Wang J., Zhang F., Lu J., *VSC-HVDC transmission line fault location based on transient characteristics*, vol. 70, no. 2, pp. 381–398 (2021), DOI: 10.24425/aee.2021.136991.

[10] Khoa N.M., Cuong M.V., Cuong H.Q., Hieu N.T.T., *Performance Comparison of Impedance-Based Fault Location Methods for Transmission Line*, International Journal of Electrical and Electronic Engineering and Telecommunications, vol. 11, no. 3, pp. 234–241 (2022), DOI: 10.18178/ijeetc.11.3.234-241.

[11] Shi S., Zhu B., Lei A., Dong X., *Fault Location for Radial Distribution Network via Topology and Reclosure-Generating Traveling Waves*, IEEE Transactions on Smart Grid, vol. 10, no. 6, pp. 6404–6413 (2019), DOI: 10.1109/TSG.2019.2904210.

[12] Salim R.H., Salim K.C.O., Bretas A.S., *Further improvements on impedance-based fault location for power distribution systems*, IET Generation, Transmission and Distribution, vol. 5, no. 4, pp. 467–478 (2011), DOI: 10.1049/iet-gtd.2010.0446.

[13] Mirshekali H., Dashti R., Keshavarz A., Torabi A.J., Shaker H.R., *A Novel Fault Location Methodology for Smart Distribution Networks*, IEEE Transactions on Smart Grid, vol. 12, no. 2, pp. 1277–1288 (2021), DOI: 10.1109/TSG.2020.3031400.

[14] Ye L., You D., Yin X., Wang K., Wu J., *An improved fault-location method for distribution system using wavelets and support vector regression*, International Journal of Electrical Power and Energy Systems, vol. 55, pp. 467–472 (2014), DOI: 10.1016/j.ijepes.2013.09.027.

[15] Pang Q., Ye L., Gao H., Li X., Wang Y., Cao T., *Multi-Timescale-Based Fault Section Location in Distribution Networks*, IEEE Access, vol. 9, pp. 148698–148709 (2021), DOI: 10.1109/ACCESS.2021.3123180.

[16] Stefanidou-Voziki P., Sapountzoglou N., Raison B., Dominguez-Garcia J.L., *A review of fault location and classification methods in distribution grids*, Electric Power Systems Research, vol. 209, p. 108031 (2022), DOI: 10.1016/j.epsr.2022.108031.

[17] Apostolopoulos C.A., Arsoniadis C.G., Georgilakis P.S., Nikolaidis V.C., *Fault location algorithms for active distribution systems utilizing two-point synchronized or unsynchronized measurements*, Sustainable Energy, Grids and Networks, vol. 32, p. 100798 (2022), DOI: 10.1016/j.segan.2022.100798.

[18] Ren J., Venkata S.S., Sortomme E., *An Accurate Synchrophasor Based Fault Location Method for Emerging Distribution Systems*, IEEE Transactions on Power Delivery, vol. 29, no. 1, pp. 297–298 (2014), DOI: 10.1109/TPWRD.2013.2288006.

[19] Aboshady F.M., Thomas D.W.P., Sumner M., *A new single end wideband impedance based fault location scheme for distribution systems*, Electric Power Systems Research, vol. 173, pp. 263–270 (2019), DOI: 10.1016/j.epsr.2019.04.034.

[20] Dashtdar M., Bajaj M., Hosseinimoghadam S.M.S., Mérshêkáér H., *Fault location in distribution network by solving the optimization problem using genetic algorithm based on the calculating voltage changes*, Soft Computing, vol. 26, pp. 8757–8783 (2022), DOI: 10.1007/s00500-022-07203-8.

[21] Ghaemi A., Safari A., Afsharirad H., Shayeghi H., *Accuracy enhance of fault classification and location in a smart distribution network based on stacked ensemble learning*, Electric Power Systems Research, vol. 205, p. 107766 (2022), DOI: 10.1016/j.epsr.2021.107766.

[22] Goudarzi M., Vahidi B., Naghizadeh R.A., Hosseinian S.H., *Improved fault location algorithm for radial distribution systems with discrete and continuous wavelet analysis*, International Journal of Electrical Power and Energy Systems, vol. 67, pp. 423–430 (2015), DOI: 10.1016/j.ijepes.2014.12.014.

[23] Hosseinimoghadam S.M.S., Dashtdar M., Dashtdar M., *Fault Location in Distribution Networks with the Presence of Distributed Generation Units Based on the Impedance Matrix*, Journal of the Institution of Engineers (India): Series B, vol. 102, pp. 227–236 (2021), DOI: 10.1007/s40031-020-00520-2.

[24] Silos-Sanchez A., Villafafila-Robles R., Lloret-Gallego P., *Novel fault location algorithm for meshed distribution networks with DERs*, Electric Power Systems Research, vol. 181, p. 106182 (2020), DOI: 10.1016/j.epsr.2019.106182.

[25] Jia K., Bi T., Ren Z., Thomas D.W.P., *High Frequency Impedance Based Fault Location in Distribution System with DGs*, IEEE Transactions on Smart Grid, vol. 9, no. 2, pp. 807–816 (2018), DOI: 10.1109/TSG.2016.2566673.

[26] Jamali S., Bahmanyar A., Bompard E., *Fault location method for distribution networks using smart meters, Measurement*, vol. 102, pp. 150–157 (2017), DOI: 10.1016/j.measurement.2017.02.008.

[27] Majidi M., Etezadi-Amoli M., *A New Fault Location Technique in Smart Distribution Networks Using Synchronized/Nonsynchronized Measurements*, IEEE Transactions on Power Delivery, vol. 33, no. 3, pp. 1358–1368 (2018), DOI: 10.1109/TPWRD.2017.2787131.

[28] Khoa N.M., Tung D.D., *Locating Fault on Transmission Line with Static Var Compensator Based on Phasor Measurement Unit*, Energies, vol. 11, no. 9, p. 2380 (2018), DOI: 10.3390/en11092380.

[29] Rui L., Nan P., Zhi Y., Zare F., *A novel single-phase-to-earth fault location method for distribution network based on zero-sequence components distribution characteristics*, International Journal of Electrical Power and Energy Systems, vol. 102, pp. 11–22 (2018), DOI: 10.1016/j.ijepes.2018.04.015.

[30] Sadeh J., Bakhshizadeh E., Kazemzadeh R., *A new fault location algorithm for radial distribution systems using modal analysis*, International Journal of Electrical Power and Energy Systems, vol. 45, no. 1, pp. 271–278 (2013), DOI: 10.1016/j.ijepes.2012.08.053.

[31] Khoa N.M., Tung D.D., *Design and Implementation of Real-time Fault Location Experimental System for Teaching and Training University Students*, International Journal of Electrical and Computer Engineering Systems, vol. 14, no. 1, pp. 109–118 (2023), DOI: 10.32985/ijeces.14.1.12.

[32] Lopes F.V., Leite E.J.S. Jr., Ribeiro J.P.G., Piardi A.B., Scheid A.V., Zat G., Espinoza R.G., *Single-ended multi-method phasor-based approach for optimized fault location on transmission lines*, Electric Power Systems Research, vol. 212, p. 108367 (2022), DOI: 10.1016/j.epsr.2022.108361.

[33] Horowitz S., Phadke A., *Power system relaying*, Tauton (USA): Research Studies Press (1995).

[34] Chen B., Yu N., Chen B., Tian C., Chen Y., Chen G., *Fault Location for Underground Cables in Ungrounded MV Distribution Networks Based on ZSC Signal Injection*, IEEE Transactions on Power Delivery, vol. 36, no. 5, pp. 2965−2977 (2021), DOI: 10.1109/TPWRD.2020.3031277.

[35] Khoa N.M., Hieu N.H., Viet D.T., *A Study of SVC's Impact Simulation and Analysis for Distance Protection Relay on Transmission Lines*, International Journal of Electrical and Computer Engineering, vol. 7, no. 4, pp. 1686–1695 (2017), DOI: 10.11591/ijece.v7i4.pp1686-1695.